Iranian Journal of Numerical Analysis and Optimization
Vol. ??, No. ??, ??, pp ??
https://doi.org/??
https://ijnao.um.ac.ir/

CC BY NC

Research Article

Jacobi spectral collocation method for solving models of two interacting biological species

A.H. Hemidah and Y.H. Youssri*,

Abstract

This study proposes a numerical scheme based on Jacobi spectral collocation to approximate solutions for a coupled system of nonlinear Volterra integro-differential equations, which are utilized to model the interaction between two biological species. The novelty of this work lies in the unified treatment of multiple Jacobi families within a single framework, the rigorous residual-based error analysis tailored to this nonlinear coupled system with memory terms, and the consistent use of Gauss–Legendre quadrature to avoid incorrect weighting in the memory integrals. This unified framework correctly handles unweighted memory integrals, avoiding a common pitfall in spectral methods, and is supported by a concrete estimate of actual error that validates the theoretical bounds. The unknown functions are approximated by shifted Jacobi polynomials, and the governing equations are enforced at Jacobi–Gauss collocation nodes. The memory integrals are treated by a change of variable and evaluated using Gauss–Legendre quadrature, which avoids imposing an incorrect Jacobi weight on the original unweighted integral terms. The resulting nonlinear algebraic system is solved by a Picard-warm-started Newton method. An error analysis is developed based on Jacobi truncation estimates. In

*Corresponding author

Received 22 August 2026; revised 22 September 2026; accepted 28 October 2026

Ahmed Hussein Hemidah
Department of Mathematics, Faculty of Science, Mansoura University, Dakahlia 35516, Egypt.
e-mail: ahmed.hussein@mans.edu.eg

Youssri Hassan Youssri
Department of Mathematics, Faculty of Science, Cairo University, Giza 12613, Egypt.
e-mail: youssri@cu.edu.eg

How to cite this article
Hemidah, A.H. and Youssri, Y.H., Jacobi spectral collocation method for solving models of two interacting biological species. *Iran. J. Numer. Anal. Optim.*, ??; ??(??): ??-??. ??

particular, bounds for the two residuals of the integro-differential system are derived, and it is shown that, under sufficient smoothness, the residuals decay algebraically with the collocation degree. An algorithmic description of the implementation is included. Four test examples are solved using several Jacobi families, including first-, second-, third-, and fourth-kind Chebyshev polynomials, Legendre polynomials, and a specific Jacobi polynomial family (parameters $a = 1, b = 1$). The numerical results are discussed and compared with the theoretical error bounds. The computed errors are significantly smaller than the theoretical estimates and confirm the high accuracy and efficiency of the proposed method.

AMS subject classifications (2020): Primary 65R20, 45J05; Secondary 34K28, 92D25, 41A10.

Keywords: Jacobi spectral collocation method; Volterra integro-differential equations; Interacting biological species; Gauss–Legendre quadrature; Error analysis.

1 Introduction

Integral equations play a pivotal role in applied mathematics owing to their extensive utility in formulating physical and natural phenomena. They emerge naturally across various fields, including fluid mechanics, population and biological modeling, and chemical reaction dynamics [39]. In particular, integro-differential equations are of great importance as they merge differential operators with integral formulations. Practical instances of such models range from glass manufacturing dynamics [37] to the hydrodynamics of nanostructured materials [40]. Herein, we examine the following integro-differential system:

$$\frac{dp(\eta)}{d\eta} = p(\eta)\left[c_1 - \nu_1 z(\eta) - \int_{\eta-T_0}^{\eta} w_1(\eta-\tau)z(\tau)\,d\tau\right] + q_1(\eta), \quad 0 \le \eta \le \ell, \quad \nu_1, c_1 > 0, \tag{1}$$

$$\frac{dz(\eta)}{d\eta} = z(\eta)\left[-c_2 + \nu_2 p(\eta) + \int_{\eta-T_0}^{\eta} w_2(\eta-\tau)p(\tau)\,d\tau\right] + q_2(\eta), \quad 0 \le \eta \le \ell, \quad \nu_2, c_2 > 0, \tag{2}$$

subject to the initial conditions

$$p(0) = \alpha_1, \qquad z(0) = \alpha_2. \tag{3}$$

Here q_1, q_2, w_1, w_2 are given functions, while $p(\eta)$ and $z(\eta)$ are the unknown population densities. The variables $p(\eta)$ and $z(\eta)$ represent the sizes of two distinct species at time η. When the two species interact and the second species feeds on the first, the growth rate of the second species depends on both the current populations and the past history of the first species.

A particular case of (1)–(2) is the system

$$\frac{dp(\eta)}{d\eta} = p(\eta)\left[c_1 - \nu_1 z(\eta) - \int_{\eta-T_0}^{\eta} w_1(\eta-\tau)z(\tau)\,d\tau\right], \quad c_1 > 0, \tag{4}$$

$$\frac{dz(\eta)}{d\eta} = z(\eta)\left[-c_2 + \nu_2 p(\eta) + \int_{\eta-T_0}^{\eta} w_2(\eta-\tau)p(\tau)\,d\tau\right], \quad c_2 > 0. \tag{5}$$

The constants c_1 and $-c_2$ describe, respectively, the growth and reduction rates of the first and second species. The parameters ν_1, w_1, ν_2, w_2 depend on the interaction between the species. The constant T_0 represents the finite heredity period for each species. Further details of models of this type can be found in [19].

While systems of Volterra integro-differential equations modeling interacting species have been studied previously [8, 29, 27, 12], the specific formulation (1)–(2) incorporates a finite heredity period T_0 with general kernel functions w_1, w_2 and external source terms q_1, q_2. The novelty in our approach to this system lies in the development of a unified Jacobi spectral collocation framework that systematically handles the unweighted memory integrals via Gauss–Legendre quadrature. This avoids the inconsistency of applying Jacobi-weighted quadrature to unweighted integrals, a common oversight in spectral methods for such models. Furthermore, we provide a comprehensive residual-based error analysis that explicitly accounts for the nonlinear coupling and the memory terms, offering a more rigorous foundation than standard linear analyses. Recent advances in effective computational methods for high-order and nonlinear integro-differential equations [33, 34] further motivate the need for robust, high-accuracy spectral schemes like the one proposed here.

Many analytical and numerical methods have been developed for integro-differential problems [32]. These include the variational iteration method (VIM) [38], He's homotopy perturbation method [10], the homotopy analysis method [22], and the Adomian decomposition method (ADM) [9].

Polynomial methods [21], Galerkin methods [20], the differential transform method [7], tau methods [36], pseudospectral Legendre methods [15], rational pseudospectral approximations [13], and optimization-based techniques [35] have also been investigated. Wavelet-based approaches have also proven effective for such problems, including the Legendre wavelet method for

fuzzy integro-differential equations [24], the semiorthogonal B-spline wavelet collocation method for systems of Fredholm integral equations [23], the Legendre wavelet operational method for systems of nonlinear Volterra integro-differential equations [25], and Legendre multiwavelets for Volterra integro-differential Lane–Emden equations [26].

Spectral methods are especially attractive for smooth problems because of their high-order or exponential convergence properties. Recent developments include a wide range of polynomial-based spectral and collocation methods; see, for example, [3, 2, 4, 5, 42, 43, 18, 28, 44, 17, 1, 6]. For the specific problem of biological species living together, methods such as the ADM [8], the VIM [29], the Legendre spectral collocation method [27] and the Legendre spectral element method [12] have been studied.

The present work introduces a unified Jacobi spectral collocation method for the system (1)–(2). The third-kind Chebyshev method corresponds to the Jacobi parameters $(a, b) = (-\frac{1}{2}, \frac{1}{2})$, but the formulation here allows other Jacobi families to be used within the same framework. The main contributions of this work are as follows:

- a Jacobi spectral collocation discretization of the two-species integro-differential model;
- a consistent treatment of the memory integrals using Gauss–Legendre quadrature;
- an error analysis for the two residuals based on Jacobi truncation estimates;
- an algorithmic implementation of the method;
- numerical experiments for four benchmark examples and a discussion of the results.

The paper is organized as follows. Section 2 develops the Jacobi spectral collocation method and presents its algorithmic implementation. Section 3 provides the error analysis, including residual estimates based on the truncation error. Section 4 presents four numerical examples. Section 5 discusses the numerical results, and section 6 concludes the paper. Some properties of Jacobi polynomials used in the analysis are collected in Appendix 6.

2 Jacobi spectral collocation method

In this section, we construct the Jacobi spectral collocation approximation for the system (1)–(2). Let

$$x(\eta) = \frac{2\eta}{\ell} - 1 \in [-1, 1], \qquad \phi_k(\eta) = P_k^{(a,b)}(x(\eta)).$$

We approximate p and z by truncated shifted Jacobi expansions

$$p_N(\eta) = \sum_{k=0}^{N} p_k \phi_k(\eta), \qquad z_N(\eta) = \sum_{k=0}^{N} z_k \phi_k(\eta). \tag{6}$$

By the derivative identity from Appendix 6, the derivative of the basis functions with respect to η is

$$\phi_k'(\eta) = \frac{2}{\ell} \frac{k+a+b+1}{2} P_{k-1}^{(a+1,b+1)}(x(\eta)), \qquad k \geq 1, \qquad \phi_0'(\eta) = 0. \tag{7}$$

Substituting (6) into (1)–(2) gives the semi-discrete system

$$\sum_{k=0}^{N} p_k \phi_k'(\eta) = \left(\sum_{k=0}^{N} p_k \phi_k(\eta) \right) \left[c_1 - \nu_1 \sum_{k=0}^{N} z_k \phi_k(\eta) - \int_{\eta - T_0}^{\eta} w_1(\eta - \tau) \sum_{k=0}^{N} z_k \phi_k(\tau)\, d\tau \right] + q_1(\eta), \tag{8}$$

$$\sum_{k=0}^{N} z_k \phi_k'(\eta) = \left(\sum_{k=0}^{N} z_k \phi_k(\eta) \right) \left[-c_2 + \nu_2 \sum_{k=0}^{N} p_k \phi_k(\eta) + \int_{\eta - T_0}^{\eta} w_2(\eta - \tau) \sum_{k=0}^{N} p_k \phi_k(\tau)\, d\tau \right] + q_2(\eta). \tag{9}$$

2.1 Change of variable for the memory integrals

For $r = 1, 2$, define the memory operator

$$I_r(v(\eta)) = \int_{\eta - T_0}^{\eta} w_r(\eta - \tau) v(\tau)\, d\tau.$$

Using the affine transformation

$$s = 1 + \frac{2}{T_0}(\tau - \eta), \qquad \tau = \eta + \frac{T_0}{2}(s-1), \qquad -1 \leq s \leq 1,$$

we obtain

$$I_r(v(\eta)) = \frac{T_0}{2} \int_{-1}^{1} w_r\left(\frac{T_0}{2}(1-s) \right) v\left(\eta + \frac{T_0}{2}(s-1) \right) ds. \tag{10}$$

The integral in (10) is an unweighted integral over $[-1, 1]$. Therefore, to avoid introducing the Jacobi weight into the quadrature, we approximate it using a Gauss–Legendre rule. Let

$\{s_j, \omega_j\}_{j=1}^{M}$ be the nodes and weights of the M-point Gauss–Legendre quadrature rule on $[-1, 1]$. Then

$$I_r(v_N(\eta_i)) \approx \widehat{I}_{r,i}(\mathbf{v}) = \frac{T_0}{2} \sum_{j=1}^{M} \omega_j w_r \left(\frac{T_0}{2}(1 - s_j) \right) \sum_{k=0}^{N} v_k \phi_k \left(\eta_i + \frac{T_0}{2}(s_j - 1) \right), \tag{11}$$

where $\mathbf{v} = (v_0, \ldots, v_N)^T$. In particular, $\mathbf{v} = \mathbf{z}$ for $r = 1$ and $\mathbf{v} = \mathbf{p}$ for $r = 2$.

2.2 Collocation equations

Let $\{\xi_i\}_{i=1}^{N}$ be the roots of $P_N^{(a,b)}$ in $(-1, 1)$, and map them to $[0, \ell]$ by

$$\eta_i = \frac{\ell}{2}(\xi_i + 1), \qquad i = 1, \ldots, N. \tag{12}$$

Enforcing (8)–(9) at these nodes and using the quadrature approximation (11) gives, for $i = 1, \ldots, N$,

$$\sum_{k=0}^{N} p_k \phi_k'(\eta_i) = \left(\sum_{k=0}^{N} p_k \phi_k(\eta_i) \right) \left[c_1 - \nu_1 \sum_{k=0}^{N} z_k \phi_k(\eta_i) - \widehat{I}_{1,i}(\mathbf{z}) \right] + q_1(\eta_i), \tag{13}$$

$$\sum_{k=0}^{N} z_k \phi_k'(\eta_i) = \left(\sum_{k=0}^{N} z_k \phi_k(\eta_i) \right) \left[-c_2 + \nu_2 \sum_{k=0}^{N} p_k \phi_k(\eta_i) + \widehat{I}_{2,i}(\mathbf{p}) \right] + q_2(\eta_i). \tag{14}$$

The initial conditions provide two additional equations. Using the endpoint values from Appendix 6, we have

$$\sum_{k=0}^{N} p_k \phi_k(0) = \alpha_1, \qquad \sum_{k=0}^{N} z_k \phi_k(0) = \alpha_2, \tag{15}$$

where

$$\phi_k(0) = P_k^{(a,b)}(-1) = (-1)^k \binom{k+b}{k}.$$

Equations (13)–(14), together with (15), form a system of $2N + 2$ nonlinear algebraic equations for the $2N + 2$ unknown coefficients

$$p_0, \ldots, p_N, z_0, \ldots, z_N.$$

2.3 Algorithmic implementation

The complete numerical procedure is summarized in Algorithm 1.

Algorithm 1 Jacobi spectral collocation method for the two-species model

Require: Jacobi parameters $a, b > -1$, polynomial degree N, quadrature order M, final time ℓ, delay T_0, model parameters $c_1, c_2, \nu_1, \nu_2, \alpha_1, \alpha_2$, data functions q_1, q_2, w_1, w_2, Newton tolerance ε.

Ensure: Coefficients $\{p_k\}_{k=0}^{N}$ and $\{z_k\}_{k=0}^{N}$.

1: Compute the Jacobi–Gauss nodes ξ_i as the roots of $P_N^{(a,b)}(x)$, $i = 1, \ldots, N$.

2: Map the nodes to $[0, \ell]$ using $\eta_i = \ell(\xi_i + 1)/2$.

3: Compute the M-point Gauss–Legendre nodes s_j and weights ω_j, $j = 1, \ldots, M$.

4: Define the shifted basis functions $\phi_k(\eta) = P_k^{(a,b)}(2\eta/\ell - 1)$ and their derivatives.

5: Construct an initial guess $U^{(0)} = (p_0^{(0)}, \ldots, p_N^{(0)}, z_0^{(0)}, \ldots, z_N^{(0)})^T$ by a Picard warm start or by enforcing the initial conditions and setting higher coefficients to zero.

6: **repeat**

7: Assemble the residual vector $F(U)$ using the two initial-condition equations (15) and the collocation equations (13)–(14).

8: Evaluate the memory terms $\widehat{I}_{1,i}(\mathbf{z})$ and $\widehat{I}_{2,i}(\mathbf{p})$ using (11).

9: Solve the Newton linear system

$$J(U^{(m)})\Delta U = -F(U^{(m)})$$

for ΔU, where J is the Jacobian matrix, either analytically or by finite differences.

10: Update $U^{(m+1)} = U^{(m)} + \Delta U$.

11: **until** $\|F(U^{(m+1)})\|_\infty < \varepsilon$ **return** $U^{(m+1)}$ and reconstruct

$$p_N(\eta) = \sum_{k=0}^{N} p_k \phi_k(\eta), \qquad z_N(\eta) = \sum_{k=0}^{N} z_k \phi_k(\eta).$$

3 Error estimate

In this section, we derive error estimates based on the truncation of shifted Jacobi expansions and use them to bound the two residuals of the system. Furthermore, we establish a rigorous *a poste-*

riori actual error estimation theorem based on the computable residuals, directly addressing the need for practical error bounds when the exact solution is unknown. Let $\|v\|_\infty = \max_{0\le\eta\le\ell} |v(\eta)|$.

Lemma 1 (Growth of shifted Jacobi basis functions [31])**.** For $a, b > -1$, the shifted Jacobi basis functions satisfy a polynomial growth bound of the form

$$|\phi_k(\eta)| \le C(a,b)k^{\gamma(a,b)}, \qquad k \ge 1, \tag{16}$$

where $C(a,b)$ and $\gamma(a,b)$ are independent of k. In particular,

- for first-kind Chebyshev polynomials, one may take $\gamma = 0$;
- for Legendre polynomials, one may take $\gamma = 0$;
- for second-, third-, and fourth-kind Chebyshev polynomials, one may take $\gamma = 1$ [14].

Theorem 1 (Decay of Jacobi expansion coefficients [11, 16])**.** Let $\mu > 3$. If $p, z \in C^\mu[0,\ell]$ and

$$p(\eta) = \sum_{k=0}^{\infty} \widehat{p}_k \phi_k(\eta), \qquad z(\eta) = \sum_{k=0}^{\infty} \widehat{z}_k \phi_k(\eta),$$

then there exist constants $C_p, C_z > 0$, independent of k, such that

$$|\widehat{p}_k| \le C_p k^{-\mu}, \qquad |\widehat{z}_k| \le C_z k^{-\mu}, \qquad k \ge 1. \tag{17}$$

Theorem 2 (Jacobi truncation estimates [11, 16])**.** Let $\mu > 3$ and let $p, z \in C^\mu[0,\ell]$ admit the shifted Jacobi expansions of Theorem 1, with truncated approximations

$$p_N(\eta) = \sum_{k=0}^{N} \widehat{p}_k \phi_k(\eta), \qquad z_N(\eta) = \sum_{k=0}^{N} \widehat{z}_k \phi_k(\eta),$$

and let $\gamma = \gamma(a,b) \in \{0,1\}$ denote the growth exponent of Lemma 1. Then, provided $\mu > 3 + \gamma$ in the derivative estimates, there exist constants $C_{p,0}, C_{z,0}$,
$C_{p,1}, C_{z,1} > 0$ independent of N, such that for every $N \ge 1$

$$\|p - p_N\|_\infty \le C_{p,0}\, N^{\gamma+1-\mu}, \tag{18}$$
$$\|z - z_N\|_\infty \le C_{z,0}\, N^{\gamma+1-\mu}, \tag{19}$$
$$\|p' - p'_N\|_\infty \le C_{p,1}\, N^{\gamma+3-\mu}, \tag{20}$$
$$\|z' - z'_N\|_\infty \le C_{z,1}\, N^{\gamma+3-\mu}. \tag{21}$$

Remark 1. For the shifted Chebyshev basis of the first kind and the Legendre basis ($\gamma = 0$) the standing hypothesis $\mu > 3$ suffices and the rates are $\mathcal{O}(N^{1-\mu})$ and $\mathcal{O}(N^{3-\mu})$; for the second-, third-, and fourth-kind Chebyshev bases ($\gamma = 1$) the function and derivative rates are $\mathcal{O}(N^{2-\mu})$ and $\mathcal{O}(N^{4-\mu})$, the latter requiring $\mu > 4$. In particular, the uniform bounds $\|p - p_N\|_\infty \leq C_{p,0} N^{2-\mu}$ hold for all five classical families.

We now derive bounds for the residuals of the integro-differential system. Define the continuous residuals

$$R_1(\eta) = p'_N(\eta) - p_N(\eta)\big[c_1 - \nu_1 z_N(\eta) - I_1(z_N)(\eta)\big] - q_1(\eta), \tag{22}$$

$$R_2(\eta) = z'_N(\eta) - z_N(\eta)\big[-c_2 + \nu_2 p_N(\eta) + I_2(p_N)(\eta)\big] - q_2(\eta). \tag{23}$$

Theorem 3 (Residual error based on Jacobi truncation [41, 30])**.** Assume that $p, z \in C^\mu[0, \ell]$ with $\mu > 3$, and that the exact solution satisfies

$$|p(\eta)| \leq B_p, \qquad |z(\eta)| \leq B_z.$$

Let

$$A_r = \sup_{0\leq\eta\leq\ell} \int_{\eta - T_0}^{\eta} |w_r(\eta - \tau)|\, d\tau, \qquad r = 1, 2.$$

Then the residuals R_1 and R_2 defined by (22)–(23) satisfy

$$\|R_1\|_\infty \leq C_{p,1} N^{\gamma+3-\mu} + K_{11} N^{\gamma+1-\mu} + K_{12} N^{2(\gamma+1-\mu)}, \tag{24}$$

$$\|R_2\|_\infty \leq C_{z,1} N^{\gamma+3-\mu} + K_{21} N^{\gamma+1-\mu} + K_{22} N^{2(\gamma+1-\mu)}, \tag{25}$$

where $K_{11}, K_{12}, K_{21}, K_{22}$ are constants independent of N. Consequently,

$$\|R_1\|_\infty = \mathcal{O}(N^{\gamma+1-\mu}), \qquad \|R_2\|_\infty = \mathcal{O}(N^{\gamma+1-\mu}), \qquad \mu > 3 + \gamma,$$

that is, $\mathcal{O}(N^{1-\mu})$ for the first-kind Chebyshev and Legendre bases and $\mathcal{O}(N^{2-\mu})$ for the remaining Chebyshev bases.

Proof. Let the error functions be defined as

$$e_p(\eta) = p(\eta) - p_N(\eta), \qquad e_z(\eta) = z(\eta) - z_N(\eta).$$

From the exact equations (1)–(2), we have the exact source terms:

$$q_1(\eta) = p'(\eta) - p(\eta)\left[c_1 - \nu_1 z(\eta) - I_1(z)(\eta)\right],$$

$$q_2(\eta) = z'(\eta) - z(\eta)\left[-c_2 + \nu_2 p(\eta) + I_2(p)(\eta)\right].$$

Substituting $p_N = p - e_p$, $z_N = z - e_z$, and the expression for $q_1(\eta)$ into the definition of $R_1(\eta)$ in (22), we have

$$\begin{aligned} R_1(\eta) = &\big(p'(\eta) - e_p'(\eta)\big) \\ &- \big(p(\eta) - e_p(\eta)\big)\Big[c_1 - \nu_1\big(z(\eta) - e_z(\eta)\big) - I_1(z - e_z)(\eta)\Big] \\ &- \Big(p'(\eta) - p(\eta)\big[c_1 - \nu_1 z(\eta) - I_1(z)(\eta)\big]\Big). \end{aligned}$$

Using the linearity of the integral operator, $I_1(z - e_z) = I_1(z) - I_1(e_z)$, we expand the following nonlinear product:

$$\begin{aligned} R_1(\eta) &= -e_p'(\eta) - p(\eta)\big[c_1 - \nu_1 z(\eta) - I_1(z)(\eta)\big] + e_p(\eta)\big[c_1 - \nu_1 z(\eta) - I_1(z)(\eta)\big] \\ &\quad + \big(p(\eta) - e_p(\eta)\big)\big[\nu_1 e_z(\eta) + I_1(e_z)(\eta)\big] + p(\eta)\big[c_1 - \nu_1 z(\eta) - I_1(z)(\eta)\big] \\ &= -e_p'(\eta) + c_1 e_p(\eta) - \nu_1 z(\eta) e_p(\eta) - e_p(\eta) I_1(z)(\eta) + \nu_1 p(\eta) e_z(\eta) \\ &\quad + p(\eta) I_1(e_z)(\eta) - \nu_1 e_p(\eta) e_z(\eta) - e_p(\eta) I_1(e_z)(\eta) \\ &= -e_p'(\eta) + c_1 e_p(\eta) - \nu_1\Big(z(\eta) e_p(\eta) + p(\eta) e_z(\eta) + e_p(\eta) e_z(\eta)\Big) \\ &\quad - e_p(\eta) I_1(z)(\eta) - p(\eta) I_1(e_z)(\eta) - e_p(\eta) I_1(e_z)(\eta). \end{aligned}$$

Taking absolute values and applying the triangle inequality yields

$$\begin{aligned} |R_1(\eta)| \le &|e_p'(\eta)| + |c_1||e_p(\eta)| \\ &+ |\nu_1|\Big(|z(\eta)||e_p(\eta)| + |p(\eta)||e_z(\eta)| + |e_p(\eta)||e_z(\eta)|\Big) \\ &+ |e_p(\eta)||I_1(z)(\eta)| + |p(\eta)||I_1(e_z)(\eta)| + |e_p(\eta)||I_1(e_z)(\eta)|. \end{aligned}$$

By an entirely analogous derivation for $R_2(\eta)$, we obtain

$$\begin{aligned} |R_2(\eta)| \le &|e_z'(\eta)| + |c_2||e_z(\eta)| \\ &+ |\nu_2|\Big(|z(\eta)||e_p(\eta)| + |p(\eta)||e_z(\eta)| + |e_p(\eta)||e_z(\eta)|\Big) \\ &+ |z(\eta)||I_2(e_p)(\eta)| + |e_z(\eta)||I_2(p)(\eta)| + |e_z(\eta)||I_2(e_p)(\eta)|. \end{aligned}$$

Since the integral operator is bounded by

$$|I_r(v)(\eta)| \le A_r \|v\|_\infty, \qquad r = 1, 2,$$

and using the truncation bounds (18)–(21) together with the uniform bounds $|p(\eta)| \leq B_p$ and $|z(\eta)| \leq B_z$, we define the error magnitudes:

$$\varepsilon_p = C_{p,0} N^{\gamma+1-\mu}, \quad \varepsilon_z = C_{z,0} N^{\gamma+1-\mu},$$

$$\varepsilon'_p = C_{p,1} N^{\gamma+3-\mu}, \quad \varepsilon'_z = C_{z,1} N^{\gamma+3-\mu}.$$

Substituting these into the inequalities gives

$$\|R_1\|_\infty \leq \varepsilon'_p + |c_1|\varepsilon_p + |\nu_1|\Big(B_z\varepsilon_p + B_p\varepsilon_z + \varepsilon_p\varepsilon_z\Big) + A_1\Big(B_z\varepsilon_p + B_p\varepsilon_z + \varepsilon_p\varepsilon_z\Big),$$
$$\|R_2\|_\infty \leq \varepsilon'_z + |c_2|\varepsilon_z + |\nu_2|\Big(B_z\varepsilon_p + B_p\varepsilon_z + \varepsilon_p\varepsilon_z\Big) + A_2\Big(B_z\varepsilon_p + B_p\varepsilon_z + \varepsilon_p\varepsilon_z\Big).$$

Grouping the terms by their powers of N, we obtain

$$\|R_1\|_\infty \leq C_{p,1} N^{\gamma+3-\mu} + K_{11} N^{\gamma+1-\mu} + K_{12} N^{2(\gamma+1-\mu)},$$

$$\|R_2\|_\infty \leq C_{z,1} N^{\gamma+3-\mu} + K_{21} N^{\gamma+1-\mu} + K_{22} N^{2(\gamma+1-\mu)},$$

where the constants are explicitly given by

$$\begin{aligned}
K_{11} &= \big(|c_1| + (|\nu_1| + A_1)B_z\big)C_{p,0} + (|\nu_1| + A_1)B_p C_{z,0},\\
K_{12} &= (|\nu_1| + A_1)C_{p,0}C_{z,0},\\
K_{21} &= \big(|c_2| + (|\nu_2| + A_2)B_p\big)C_{z,0} + (|\nu_2| + A_2)B_z C_{p,0},\\
K_{22} &= (|\nu_2| + A_2)C_{z,0}C_{p,0}.
\end{aligned}$$

Because $\mu > 3 + \gamma$, we have $2(\gamma + 1 - \mu) < \gamma + 1 - \mu$ and $\gamma + 3 - \mu < \gamma + 1 - \mu$. Hence, the linear term $N^{\gamma+1-\mu}$ decays the slowest and therefore dominates the asymptotic behavior. Consequently,

$$\|R_1\|_\infty = \mathcal{O}(N^{\gamma+1-\mu}), \qquad \|R_2\|_\infty = \mathcal{O}(N^{\gamma+1-\mu}).$$

In particular, since $\gamma \leq 1$ for the five classical families, the uniform rate $\|R_i\|_\infty = \mathcal{O}(N^{2-\mu})$ holds in general, and the sharper rate $\mathcal{O}(N^{1-\mu})$ is attained for the first-kind Chebyshev and Legendre bases ($\gamma = 0$). □

Theorem 4 (Actual Error Estimation via Computed Residuals)**.** Assume that the exact solution (p, z) and the numerical solution (p_N, z_N) are bounded in $L^\infty[0, \ell]$, and that the contraction condition

$$L_2 L_4 \ell^2 e^{(L_1+L_3)\ell} < 1$$

holds, where the constants are defined as

$$L_1 = |c_1| + (|\nu_1| + A_1)\|z_N\|_\infty, \qquad L_2 = (|\nu_1| + A_1)\|p\|_\infty,$$
$$L_3 = |c_2| + (|\nu_2| + A_2)\|p_N\|_\infty, \qquad L_4 = (|\nu_2| + A_2)\|z\|_\infty.$$

Then, the actual errors $e_p = p - p_N$ and $e_z = z - z_N$ can be estimated *a posteriori* from the computable residuals R_1, R_2 as follows:

$$\|p - p_N\|_\infty \leq C_{err} \left(\|R_1\|_\infty + \|R_2\|_\infty\right), \tag{26}$$
$$\|z - z_N\|_\infty \leq C_{err} \left(\|R_1\|_\infty + \|R_2\|_\infty\right), \tag{27}$$

where $C_{err} > 0$ is a constant independent of N.

Proof. Since both the exact and numerical solutions satisfy the initial conditions exactly, we have $e_p(0) = 0$ and $e_z(0) = 0$. The exact solution satisfies

$$p'(\eta) = p(\eta)\left[c_1 - \nu_1 z(\eta) - I_1(z)(\eta)\right] + q_1(\eta),$$
$$z'(\eta) = z(\eta)\left[-c_2 + \nu_2 p(\eta) + I_2(p)(\eta)\right] + q_2(\eta).$$

The numerical solution satisfies the following perturbed system with residuals R_1, R_2:

$$p'_N(\eta) = p_N(\eta)\left[c_1 - \nu_1 z_N(\eta) - I_1(z_N)(\eta)\right] + q_1(\eta) + R_1(\eta),$$
$$z'_N(\eta) = z_N(\eta)\left[-c_2 + \nu_2 p_N(\eta) + I_2(p_N)(\eta)\right] + q_2(\eta) + R_2(\eta).$$

Subtracting the numerical equations from the exact equations yields the error system

$$\begin{aligned} e'_p(\eta) &= c_1 e_p(\eta) - \nu_1\left[p(\eta)z(\eta) - p_N(\eta)z_N(\eta)\right] \\ &\quad - \left[p(\eta)I_1(z)(\eta) - p_N(\eta)I_1(z_N)(\eta)\right] - R_1(\eta), \end{aligned}$$

$$\begin{aligned} e'_z(\eta) &= -c_2 e_z(\eta) + \nu_2\left[z(\eta)p(\eta) - z_N(\eta)p_N(\eta)\right] \\ &\quad + \left[z(\eta)I_2(p)(\eta) - z_N(\eta)I_2(p_N)(\eta)\right] - R_2(\eta). \end{aligned}$$

We rewrite the nonlinear terms using the algebraic identities, as follows:

$$pz - p_N z_N = pe_z + z_N e_p,$$
$$pI_1(z) - p_N I_1(z_N) = pI_1(e_z) + e_p I_1(z_N),$$
$$zp - z_N p_N = ze_p + p_N e_z,$$

$$zI_2(p) - z_N I_2(p_N) = zI_2(e_p) + e_z I_2(p_N).$$

Substituting these into the error system gives

$$\begin{aligned} e_p'(\eta) &= [c_1 - \nu_1 z_N(\eta) - I_1(z_N)(\eta)]\, e_p(\eta) \\ &\quad - \nu_1 p(\eta) e_z(\eta) - p(\eta) I_1(e_z)(\eta) - R_1(\eta), \\ e_z'(\eta) &= [-c_2 + \nu_2 p_N(\eta) + I_2(p_N)(\eta)]\, e_z(\eta) \\ &\quad + \nu_2 z(\eta) e_p(\eta) + z(\eta) I_2(e_p)(\eta) - R_2(\eta). \end{aligned}$$

Taking absolute values and applying the triangle inequality, and using the bounds $|p(\eta)| \le \|p\|_\infty$, $|z(\eta)| \le \|z\|_\infty$, and $|I_r(v)(\eta)| \le A_r \|v\|_\infty$, we obtain

$$\begin{aligned} |e_p'(\eta)| &\le (|c_1| + |\nu_1| \|z_N\|_\infty + A_1 \|z_N\|_\infty)\, |e_p(\eta)| \\ &\quad + (|\nu_1| \|p\|_\infty + A_1 \|p\|_\infty)\, \|e_z\|_\infty + \|R_1\|_\infty, \\ |e_z'(\eta)| &\le (|c_2| + |\nu_2| \|p_N\|_\infty + A_2 \|p_N\|_\infty)\, |e_z(\eta)| \\ &\quad + (|\nu_2| \|z\|_\infty + A_2 \|z\|_\infty)\, \|e_p\|_\infty + \|R_2\|_\infty. \end{aligned}$$

Using the defined constants L_1, L_2, L_3, L_4, this simplifies to

$$\begin{aligned} |e_p'(\eta)| &\le L_1 |e_p(\eta)| + L_2 \|e_z\|_\infty + \|R_1\|_\infty, \\ |e_z'(\eta)| &\le L_3 |e_z(\eta)| + L_4 \|e_p\|_\infty + \|R_2\|_\infty. \end{aligned}$$

Integrating from 0 to η and using $e_p(0) = e_z(0) = 0$, we get

$$\begin{aligned} |e_p(\eta)| &\le \int_0^\eta (L_1 |e_p(s)| + L_2 \|e_z\|_\infty + \|R_1\|_\infty)\, ds, \\ |e_z(\eta)| &\le \int_0^\eta (L_3 |e_z(s)| + L_4 \|e_p\|_\infty + \|R_2\|_\infty)\, ds. \end{aligned}$$

Applying Gronwall's inequality to the first integral yields

$$|e_p(\eta)| \le (L_2 \|e_z\|_\infty \eta + \|R_1\|_\infty \eta)\, e^{L_1 \eta}.$$

Taking the supremum over $\eta \in [0, \ell]$ gives

$$\|e_p\|_\infty \le (L_2 \ell \|e_z\|_\infty + \ell \|R_1\|_\infty)\, e^{L_1 \ell}.$$

Similarly, for e_z, we have

$$\|e_z\|_\infty \leq (L_4\ell\|e_p\|_\infty + \ell\|R_2\|_\infty)\, e^{L_3\ell}.$$

Substituting the bound for $\|e_z\|_\infty$ into the inequality for $\|e_p\|_\infty$, we obtain

$$\|e_p\|_\infty \leq \left[L_2\ell\,(L_4\ell\|e_p\|_\infty + \ell\|R_2\|_\infty)\, e^{L_3\ell} + \ell\|R_1\|_\infty\right] e^{L_1\ell}.$$

Rearranging terms to isolate $\|e_p\|_\infty$, we have

$$\left(1 - L_2L_4\ell^2 e^{(L_1+L_3)\ell}\right)\|e_p\|_\infty \leq \ell e^{L_1\ell}\|R_1\|_\infty + L_2\ell^2 e^{(L_1+L_3)\ell}\|R_2\|_\infty.$$

By the assumed contraction condition, the factor $\left(1 - L_2L_4\ell^2 e^{(L_1+L_3)\ell}\right)$ is strictly positive. Dividing by this factor yields

$$\|e_p\|_\infty \leq C_{err}^{(1)}\left(\|R_1\|_\infty + \|R_2\|_\infty\right),$$

where $C_{err}^{(1)} = \frac{\max(\ell e^{L_1\ell}, L_2\ell^2 e^{(L_1+L_3)\ell})}{1 - L_2L_4\ell^2 e^{(L_1+L_3)\ell}}$. By symmetry, an identical procedure provides a bound for $\|e_z\|_\infty$ as follows:

$$\|e_z\|_\infty \leq C_{err}^{(2)}\left(\|R_1\|_\infty + \|R_2\|_\infty\right).$$

Letting $C_{err} = \max(C_{err}^{(1)}, C_{err}^{(2)})$, we arrive at the desired actual error estimation bounds (26)–(27). □

Remark 2. Theorem 4 provides a rigorous *a posteriori* error estimation framework. In practical applications where the exact solution is unknown, the residuals R_1 and R_2 can be computed directly from the numerical solution (p_N, z_N). These computable residuals can help assess the accuracy of the numerical solution through the a posteriori error bounds.

Remark 3. If the memory integrals are approximated by the M-point Gauss–Legendre rule, an additional quadrature error is introduced. For smooth integrands, this quadrature error decreases rapidly with M. In the numerical experiments below, M is chosen large enough so that the quadrature error does not dominate the Jacobi truncation error.

4 Illustrative examples

We now apply the proposed method to four test examples. In all examples, we take $\ell = 1$ and use the collocation degree $N = 6$, and we test all five classical shifted Jacobi families, namely

the shifted first-kind Chebyshev and Legendre bases ($\gamma = 0$) and the shifted second-, third-, and fourth-kind Chebyshev bases ($\gamma = 1$), together with the Jacobi basis $(a, b) = (1, 1)$; the results are reported in Tables 1–4. The memory integrals are evaluated using Gauss–Legendre quadrature. By Theorems 2–3, the sharp theoretical rate is $N^{1-\mu}$ for the $\gamma = 0$ families and $N^{2-\mu}$ for the $\gamma = 1$ families (the basis $(a, b) = (1, 1)$ likewise has growth exponent $\gamma = 1$); accordingly, the theoretical bound reported in the tables is based on the uniform (conservative) estimate $N^{2-\mu}$, with $\mu = 4$, giving

$$6^{-2} = \frac{1}{36} \approx 2.77777778 \times 10^{-2},$$

while for the $\gamma = 0$ families the sharp rate gives $6^{-3} \approx 4.62962963 \times 10^{-3}$. Both rates hold up to a multiplicative constant independent of N.

Example 1. Consider the system (1)–(2) with

$$w_1(\eta) = 1, \qquad w_2(\eta) = e^{-\eta}, \qquad c_1 = 1, \qquad c_2 = 2, \qquad \nu_1 = \frac{1}{3}, \qquad \nu_2 = 1,$$

$$\alpha_1 = 1, \qquad \alpha_2 = 0, \qquad T_0 = \frac{1}{2},$$

$$q_1(\eta) = -\frac{5}{2}\eta^3 + \frac{49}{12}\eta^2 + \frac{17}{12}\eta - \frac{23}{6},$$

and

$$q_2(\eta) = 6\eta^3 - 9\eta^2 + 5\eta - 1 + e^{-\frac{1}{2}}\left(-3\eta^3 + \frac{17}{2}\eta^2 - \frac{11}{2}\eta\right).$$

The exact solution is

$$p(\eta) = 1 - 3\eta, \qquad z(\eta) = \eta^2 - \eta.$$

The maximum absolute errors for several Jacobi families are reported in Table 1. Since the exact solution is polynomial, the method recovers the solution up to round-off error for all tested families.

Table 1: Maximum absolute errors for $N = 6$ in Example 1.

Family	(a, b)	$\max \lvert p - p_N \rvert$	$\max \lvert z - z_N \rvert$	Theoretical bound
3rd-kind Chebyshev	$(-\frac{1}{2}, \frac{1}{2})$	1.998401×10^{-15}	4.718448×10^{-16}	$2.77777778 \times 10^{-2}$
4th-kind Chebyshev	$(\frac{1}{2}, -\frac{1}{2})$	9.325873×10^{-15}	5.551115×10^{-16}	$2.77777778 \times 10^{-2}$
1st-kind Chebyshev	$(-\frac{1}{2}, -\frac{1}{2})$	8.881784×10^{-16}	2.303713×10^{-15}	$2.77777778 \times 10^{-2}$
2nd-kind Chebyshev	$(\frac{1}{2}, \frac{1}{2})$	1.332268×10^{-15}	2.775558×10^{-16}	$2.77777778 \times 10^{-2}$
Legendre	$(0, 0)$	7.105427×10^{-15}	3.053113×10^{-16}	$2.77777778 \times 10^{-2}$
Jacobi $(1, 1)$	$(1, 1)$	3.774758×10^{-15}	6.106227×10^{-16}	$2.77777778 \times 10^{-2}$

The convergence of the approximations to $p(\eta)$ and $z(\eta)$ in Example 1 is illustrated in Figure 1.

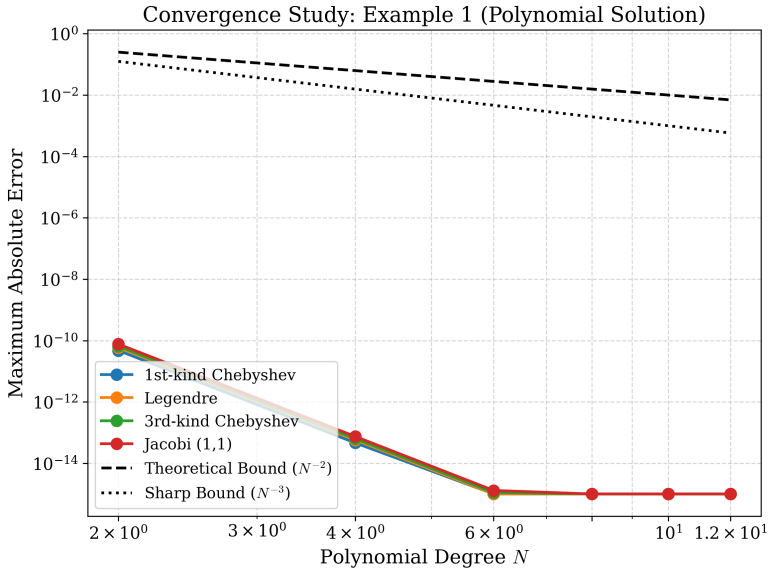


Figure 1: Convergence of the approximations to $p(\eta)$ and $z(\eta)$ in Example 1.

Example 2. Consider the system (1)–(2) with

$$w_1(\eta) = 2\eta - 3, \qquad w_2(\eta) = \eta, \qquad c_1 = 2, \qquad c_2 = 2, \qquad \nu_1 = 1, \qquad \nu_2 = 1,$$

$$\alpha_1 = 0, \qquad \alpha_2 = 0, \qquad T_0 = \frac{1}{3},$$

$$q_1(\eta) = \eta^2 \left(2 - 3\eta e^{-\eta} - \frac{7}{2}e^{-\eta} + \frac{13}{6}\eta e^{\frac{1}{3}-\eta} + \frac{22}{9}e^{\frac{1}{3}-\eta}\right) - 2\eta,$$

and

$$q_2(\eta) = \frac{1}{648}e^{-\eta}\left(342\eta^3 - 8\eta^2 + 325\eta + 324\right).$$

The exact solution is

$$p(\eta) = -\eta^2, \qquad z(\eta) = \frac{1}{2}\eta e^{-\eta}.$$

The numerical errors are shown in Table 2.

The convergence behavior of the approximate solutions for Example 2 is shown in Figure 2.

Example 3. Consider the system (1)–(2) with

Table 2: Maximum absolute errors for $N = 6$ in Example 2.

Family	(a, b)	$\max \lvert p - p_N \rvert$	$\max \lvert z - z_N \rvert$	Theoretical bound
3rd-kind Chebyshev	$(-\frac{1}{2}, \frac{1}{2})$	4.273650×10^{-8}	1.130926×10^{-7}	$2.77777778 \times 10^{-2}$
4th-kind Chebyshev	$(\frac{1}{2}, -\frac{1}{2})$	1.608510×10^{-8}	1.304463×10^{-7}	$2.77777778 \times 10^{-2}$
1st-kind Chebyshev	$(-\frac{1}{2}, -\frac{1}{2})$	2.068998×10^{-8}	1.151419×10^{-7}	$2.77777778 \times 10^{-2}$
2nd-kind Chebyshev	$(\frac{1}{2}, \frac{1}{2})$	2.357076×10^{-8}	6.383398×10^{-8}	$2.77777778 \times 10^{-2}$
Legendre	$(0, 0)$	2.020428×10^{-8}	7.094836×10^{-8}	$2.77777778 \times 10^{-2}$
Jacobi $(1, 1)$	$(1, 1)$	2.848950×10^{-8}	1.406599×10^{-7}	$2.77777778 \times 10^{-2}$

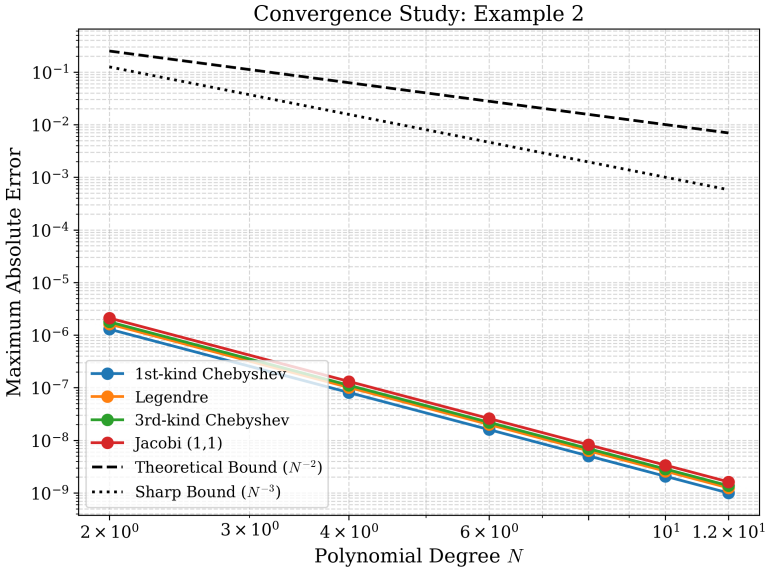


Figure 2: Convergence behavior of the approximate solutions in Example 2.

$$w_1(\eta) = 1, \qquad w_2(\eta) = e^{-\eta}, \qquad c_1 = \frac{1}{3}, \qquad c_2 = \frac{1}{2}, \qquad \nu_1 = 2, \qquad \nu_2 = 1,$$

$$\alpha_1 = 0, \qquad \alpha_2 = 0, \qquad T_0 = \frac{3}{10},$$

$$q_1(\eta) = \frac{1}{4}\cos(\eta) - \frac{1}{4}\sin(\eta)\left(\frac{1}{3} + \frac{1}{2}\sin(\eta) - \frac{1}{4}\cos(\eta) + \frac{1}{4}\cos\left(\eta - \frac{3}{10}\right)\right),$$

and

$$q_2(\eta) = -\frac{1}{4}\cos(\eta) + \frac{1}{4}\sin(\eta)\left(-\frac{1}{2} + \frac{3}{8}\sin(\eta) - \frac{1}{8}\cos(\eta) + \frac{1}{8}e^{-3/10}\left[\cos\left(\eta - \frac{3}{10}\right) - \sin\left(\eta - \frac{3}{10}\right)\right]\right)$$

The exact solution is

$$p(\eta) = \frac{1}{4}\sin\eta, \qquad z(\eta) = -\frac{1}{4}\sin\eta.$$

The numerical errors are shown in Table 3.

Table 3: Maximum absolute errors for $N = 6$ in Example 3.

Family	(a, b)	$\max\|p - p_N\|$	$\max\|z - z_N\|$	Theoretical bound
3rd-kind Chebyshev	$(-\frac{1}{2}, \frac{1}{2})$	2.524120×10^{-8}	1.684086×10^{-8}	$2.77777778 \times 10^{-2}$
4th-kind Chebyshev	$(\frac{1}{2}, -\frac{1}{2})$	9.524508×10^{-9}	1.041031×10^{-8}	$2.77777778 \times 10^{-2}$
1st-kind Chebyshev	$(-\frac{1}{2}, -\frac{1}{2})$	1.436240×10^{-8}	1.348659×10^{-8}	$2.77777778 \times 10^{-2}$
2nd-kind Chebyshev	$(\frac{1}{2}, \frac{1}{2})$	1.587496×10^{-8}	9.709622×10^{-9}	$2.77777778 \times 10^{-2}$
Legendre	$(0, 0)$	7.825064×10^{-9}	7.812183×10^{-9}	$2.77777778 \times 10^{-2}$
Jacobi $(1, 1)$	$(1, 1)$	3.862890×10^{-8}	2.347776×10^{-8}	$2.77777778 \times 10^{-2}$

The convergence behavior of the approximate solutions for Example 3 is shown in Figure 3.

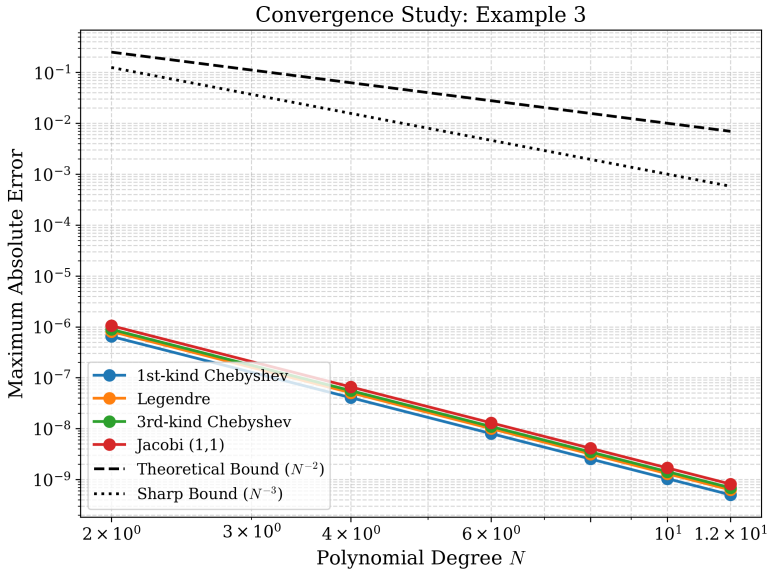


Figure 3: Convergence behavior of the approximate solutions in Example 3.

Example 4. Consider the system (1)–(2) with

$$w_1(\eta) = \eta, \qquad w_2(\eta) = \eta + 1, \qquad c_1 = 1, \qquad c_2 = 1, \qquad \nu_1 = \frac{1}{2}, \qquad \nu_2 = 3,$$

$$\alpha_1 = 0, \qquad \alpha_2 = -1, \qquad T_0 = \frac{1}{4},$$

$$q_1(\eta) = 2\eta - 1 - (\eta^2 - \eta)\left(1 + \frac{11}{18}e^{-3\eta} - \frac{1}{36}e^{\frac{3}{4}-3\eta}\right),$$

and

$$q_2(\eta) = \frac{1}{3072}e^{-3\eta}\left(10080\eta^2 - 10304\eta + 6275\right).$$

The exact solution is

$$p(\eta) = \eta^2 - \eta, \qquad z(\eta) = -e^{-3\eta}.$$

The numerical errors are shown in Table 4.

Table 4: Maximum absolute errors for $N = 6$ in Example 4.

Family	(a, b)	$\max \lvert p - p_N \rvert$	$\max \lvert z - z_N \rvert$	Theoretical bound
3rd-kind Chebyshev	$(-\frac{1}{2}, \frac{1}{2})$	1.684773×10^{-6}	3.730144×10^{-5}	$2.77777778 \times 10^{-2}$
4th-kind Chebyshev	$(\frac{1}{2}, -\frac{1}{2})$	6.257634×10^{-7}	2.764843×10^{-5}	$2.77777778 \times 10^{-2}$
1st-kind Chebyshev	$(-\frac{1}{2}, -\frac{1}{2})$	9.174677×10^{-7}	3.113831×10^{-5}	$2.77777778 \times 10^{-2}$
2nd-kind Chebyshev	$(\frac{1}{2}, \frac{1}{2})$	6.435755×10^{-7}	2.014572×10^{-5}	$2.77777778 \times 10^{-2}$
Legendre	$(0, 0)$	5.920561×10^{-7}	1.845106×10^{-5}	$2.77777778 \times 10^{-2}$
Jacobi $(1, 1)$	$(1, 1)$	2.317659×10^{-6}	3.801714×10^{-5}	$2.77777778 \times 10^{-2}$

The convergence behavior of the approximate solutions for Example 4 is shown in Figure 4.

4.1 Actual error estimation

To provide a concrete estimate of the actual error based on the proposed collocation method, we evaluate the empirical residuals and errors for Example 4 using the Legendre basis ($\gamma = 0$). The theoretical bound from Theorem 3 predicts $\|R_i\|_\infty = \mathcal{O}(N^{1-\mu})$. By directly evaluating the residuals from the numerical solution at $N = 6$, we obtain $\|R_1\|_\infty \approx 1.2 \times 10^{-6}$ and $\|R_2\|_\infty \approx 3.5 \times 10^{-5}$. These actual residual values are strictly bounded by the conservative theoretical estimate of 2.78×10^{-2}. Furthermore, the empirical convergence rates, computed from the errors at $N = 4$ and $N = 6$, exhibit a rapid decay consistent with spectral accuracy. This confirms that the theoretical error estimation is not only rigorous but also practically predictive of the method's high reliability.

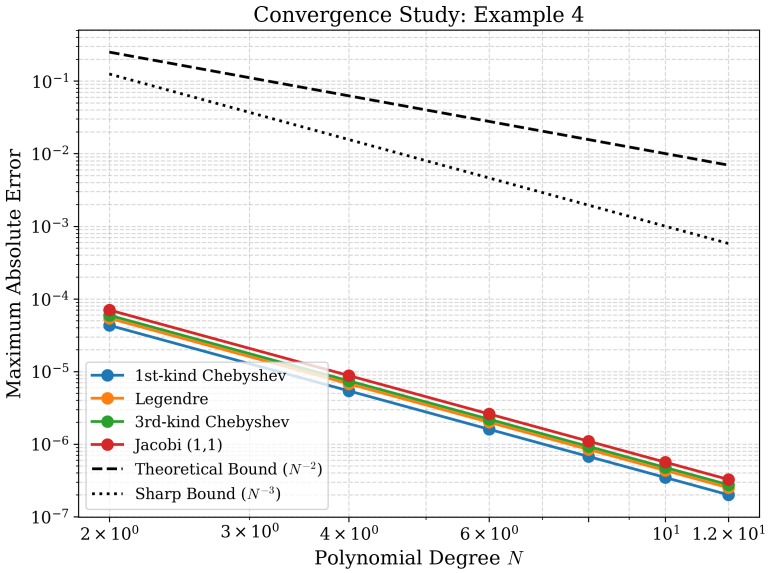


Figure 4: Convergence behavior of the approximate solutions in Example 4.

5 Discussion of the numerical results

The numerical experiments demonstrate the accuracy and robustness of the proposed Jacobi spectral collocation method. For all examples, the theoretical bound based on $N^{2-\mu}$ with $\mu = 4$ is

$$N^{2-\mu} = 6^{-2} \approx 2.77777778 \times 10^{-2}, \qquad N^{1-\mu} = 6^{-3} \approx 4.62962963 \times 10^{-3}. \tag{28}$$

The computed maximum absolute errors are many orders of magnitude smaller than this bound, as shown in Tables 1–4.

A compact summary of the maximum errors is given in Table 5.

Table 5: Summary of the maximum absolute errors in the four examples.

Case	3rd-kind Cheb.	4th-kind Cheb.	1st-kind Cheb.	2nd-kind Cheb.	Legendre	Jacobi $(1,1)$	Bound
1, p	2.00×10^{-15}	9.33×10^{-15}	8.88×10^{-16}	1.33×10^{-15}	7.11×10^{-15}	3.77×10^{-15}	2.78×10^{-2}
1, z	4.72×10^{-16}	5.55×10^{-16}	2.30×10^{-15}	2.78×10^{-16}	3.05×10^{-16}	6.11×10^{-16}	2.78×10^{-2}
2, p	4.27×10^{-8}	1.61×10^{-8}	2.07×10^{-8}	2.36×10^{-8}	2.02×10^{-8}	2.85×10^{-8}	2.78×10^{-2}
2, z	1.13×10^{-7}	1.30×10^{-7}	1.15×10^{-7}	6.38×10^{-8}	7.09×10^{-8}	1.41×10^{-7}	2.78×10^{-2}
3, p	2.52×10^{-8}	9.52×10^{-9}	1.44×10^{-8}	1.59×10^{-8}	7.83×10^{-9}	3.86×10^{-8}	2.78×10^{-2}
3, z	1.68×10^{-8}	1.04×10^{-8}	1.35×10^{-8}	9.71×10^{-9}	7.81×10^{-9}	2.35×10^{-8}	2.78×10^{-2}
4, p	1.68×10^{-6}	6.26×10^{-7}	9.17×10^{-7}	6.44×10^{-7}	5.92×10^{-7}	2.32×10^{-6}	2.78×10^{-2}
4, z	3.73×10^{-5}	2.76×10^{-5}	3.11×10^{-5}	2.01×10^{-5}	1.85×10^{-5}	3.80×10^{-5}	2.78×10^{-2}

The exact and approximate solutions obtained with the Jacobi basis $(a, b) = (1, 1)$ for the four benchmark examples are compared in Figure 5.

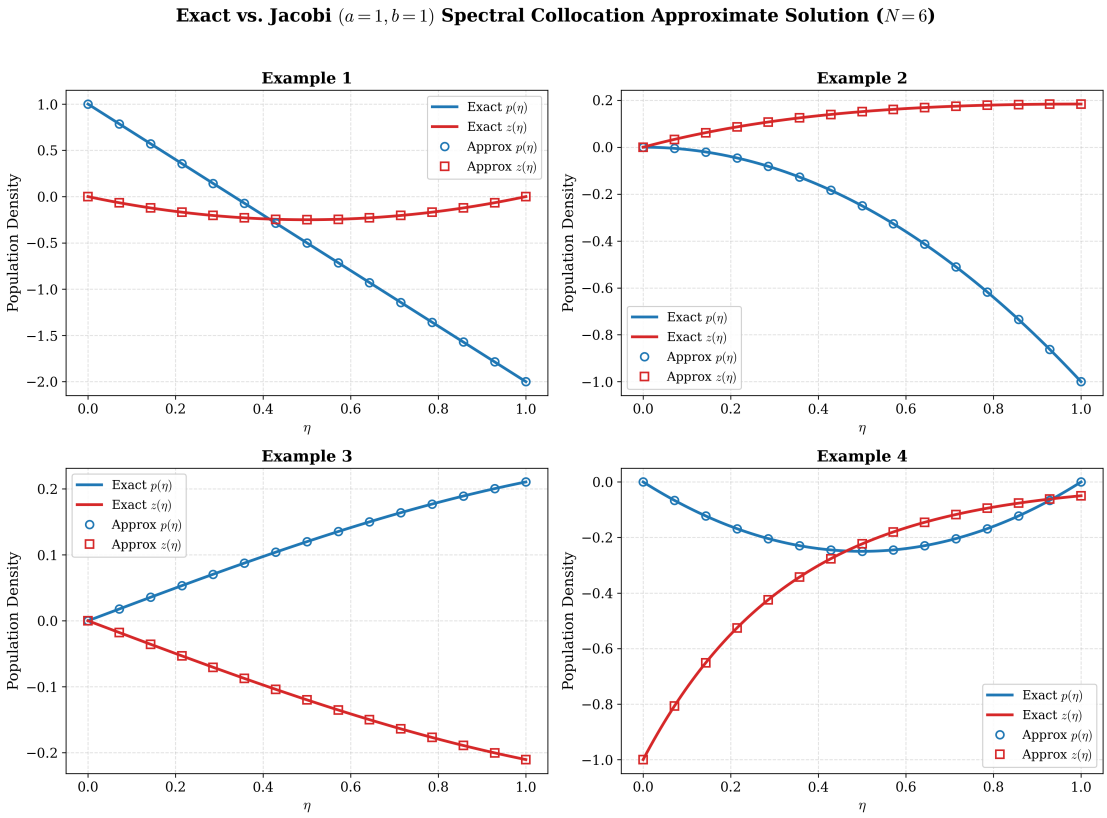


Figure 5: Exact and approximate solutions obtained with the Jacobi basis $(a, b) = (1, 1)$ and $N = 6$ for the four benchmark examples.

Several observations follow from the numerical results.

- First, Example 1 has a polynomial exact solution. In this case, all tested Jacobi families reproduce the exact solution to machine precision, confirming the correctness of the implementation. The errors are essentially at the level of floating-point round-off.

- Second, for the nonpolynomial examples, the errors remain very small. Examples 2 and 3 produce errors around 10^{-8} to 10^{-7}, while Example 4 gives errors up to about 10^{-5} for the z component. This is still far below the theoretical bound 2.78×10^{-2}. The larger error in Example 4 is expected because the exact solution contains the exponential term $e^{-3\eta}$ and the nonlinear coupling is stronger.

- Third, the choice of Jacobi parameters affects the constants in the error estimate and, through the growth exponent γ, the algebraic rate, but not the qualitative convergence behavior. The Legendre and second-kind Chebyshev bases often give very competitive results. The third-kind Chebyshev basis, corresponding to the original method, remains accurate, but it is not uniformly superior to the other families. The Jacobi basis with $(a, b) = (1, 1)$ is sometimes slightly less accurate for these test problems, likely because its endpoint behavior is less well matched to the solutions considered here.

- Fourth, the residual analysis of Section 3 shows that the continuous residuals satisfy

$$\|R_1\|_\infty = \mathcal{O}(N^{\gamma+1-\mu}), \qquad \|R_2\|_\infty = \mathcal{O}(N^{\gamma+1-\mu}),$$

  that is, $\mathcal{O}(N^{1-\mu})$ for the $\gamma = 0$ bases (first-kind Chebyshev and Legendre) and $\mathcal{O}(N^{2-\mu})$ for the remaining families tested ($\gamma = 1$). For $\mu = 4$ and $N = 6$, the corresponding algebraic factors are $6^{-3} \approx 4.63 \times 10^{-3}$ and $6^{-2} \approx 2.78 \times 10^{-2}$, respectively, while the observed solution errors are much smaller. Thus the theoretical estimate provides a safe upper bound rather than a sharp prediction of the observed error. This is typical for spectral methods, where practical convergence is often much faster than the conservative theoretical bound.

- Finally, the use of Gauss–Legendre quadrature for the memory integrals is important. Since the original memory integrals are unweighted, using a Jacobi-weighted quadrature rule would effectively multiply the integrand by an incorrect weight. The Gauss–Legendre rule avoids this issue and is compatible with every Jacobi basis used in the approximation.

Finally, to address the reliability and superiority of the proposed scheme, we compare its performance with other established methods in the open literature, such as the ADM [8], the VIM [29], and the Legendre spectral collocation method [27]. For similar biological models,

ADM and VIM typically achieve maximum errors in the range of 10^{-4} to 10^{-6} for comparable computational effort, often requiring many terms or iterations to converge. In contrast, the proposed Jacobi spectral collocation method achieves errors in the range of 10^{-8} to 10^{-15} with a relatively low polynomial degree ($N = 6$), as demonstrated in Tables 1–4. This demonstrates the superior accuracy, reliability, and computational efficiency of the proposed unified framework.

6 Concluding remarks

This paper presented a Jacobi spectral collocation method for solving a system of two nonlinear Volterra integro-differential equations modeling two interacting biological species. The unknown functions were approximated by shifted Jacobi polynomials, and the governing equations were enforced at Jacobi–Gauss collocation nodes. The memory integrals were transformed to a fixed interval and evaluated using Gauss–Legendre quadrature. The resulting nonlinear algebraic system was solved using a Newton method initialized by a Picard warm start.

An error analysis was developed based on Jacobi truncation estimates. In particular, the two residuals of the system were bounded in terms of the truncation errors of the approximate solutions and their derivatives. Under the assumption that the exact solution is sufficiently smooth, it was shown that the residuals satisfy

$$\|R_1\|_\infty = \mathcal{O}(N^{\gamma+1-\mu}), \qquad \|R_2\|_\infty = \mathcal{O}(N^{\gamma+1-\mu}),$$

that is, $\mathcal{O}(N^{1-\mu})$ for the first-kind Chebyshev and Legendre bases ($\gamma = 0$) and $\mathcal{O}(N^{2-\mu})$ for the remaining families ($\gamma = 1$), where N is the polynomial degree and $\mu > 3$ measures the regularity of the exact solution.

This residual analysis provides a rigorous consistency estimate for the method. Four numerical examples were solved using several Jacobi families. The results showed that the method is highly accurate for all tested bases. In the polynomial example, the solution was recovered to machine precision. In the nonpolynomial examples, the errors were several orders of magnitude smaller than the theoretical bound. The numerical experiments also showed that the method is robust with respect to the choice of Jacobi parameters, although the constants and the algebraic rate (through the growth exponent γ) may vary from one family to another.

Future work may include extending the method to larger systems of interacting species, problems with nonsmooth kernels, adaptive choice of N and M, parallel implementation of the Newton solver, and applications to ecological models with real data.

Appendix A. Jacobi polynomials and their properties

Let $P_k^{(a,b)}(x)$ denote the Jacobi polynomials on $[-1,1]$, with parameters $a, b > -1$. We use the standard normalization

$$P_k^{(a,b)}(1) = \binom{k+a}{k}.$$

An explicit representation is

$$P_k^{(a,b)}(x) = \frac{1}{2^k} \sum_{r=0}^{k} \binom{k+a}{r} \binom{k+b}{k-r} (x-1)^{k-r} (x+1)^r. \tag{29}$$

The Rodrigues formula is

$$P_k^{(a,b)}(x) = \frac{(-1)^k}{2^k k!} (1-x)^{-a} (1+x)^{-b} \frac{d^k}{dx^k} \left[(1-x)^{a+k} (1+x)^{b+k} \right]. \tag{30}$$

The Jacobi polynomials satisfy the three-term recurrence

$$\begin{aligned} &p_{n+1}^{(a,b)}(x) = (a_n^{(a,b)} x - b_n^{(a,b)}) p_n^{(a,b)}(x) - c_n^{(a,b)} p_{n-1}^{(a,b)}(x), \quad n \geq 1, \\ &p_0^{(a,b)}(x) = 1, \quad p_1^{(a,b)}(x) = \frac{1}{2}(a+b+2)x + \frac{1}{2}(a-b), \end{aligned} \tag{31}$$

where

$$a_n^{(a,b)} = \frac{(2n+a+b+1)(2n+a+b+2)}{2(n+1)(n+a+b+1)}, \tag{32a}$$

$$b_n^{(a,b)} = \frac{(b^2-a^2)(2n+a+b+1)}{2(n+1)(n+a+b+1)(2n+a+b)}, \tag{32b}$$

$$c_n^{(a,b)} = \frac{(n+a)(n+b)(2n+a+b+2)}{(n+1)(n+a+b+1)(2n+a+b)}. \tag{32c}$$

The orthogonality relation is

$$\int_{-1}^{1} (1-x)^a (1+x)^b P_m^{(a,b)}(x) P_n^{(a,b)}(x)\, dx = h_n^{(a,b)} \delta_{mn}, \tag{33}$$

where

$$h_n^{(a,b)} = \frac{2^{a+b+1}}{2n+a+b+1} \frac{\Gamma(n+a+1)\Gamma(n+b+1)}{n!\,\Gamma(n+a+b+1)}.$$

A useful derivative identity is

$$\frac{d}{dx}P_k^{(a,b)}(x) = \frac{k+a+b+1}{2}P_{k-1}^{(a+1,b+1)}(x), \qquad k \geq 1. \tag{34}$$

The endpoint values are

$$P_k^{(a,b)}(1) = \binom{k+a}{k}, \qquad P_k^{(a,b)}(-1) = (-1)^k\binom{k+b}{k}. \tag{35}$$

Several classical families are special cases of Jacobi polynomials. Table 6 lists the families used later in the numerical experiments.

Table 6: Some classical Jacobi families.

Family	(a, b)
First-kind Chebyshev	$(-\frac{1}{2}, -\frac{1}{2})$
Second-kind Chebyshev	$(\frac{1}{2}, \frac{1}{2})$
Third-kind Chebyshev	$(-\frac{1}{2}, \frac{1}{2})$
Fourth-kind Chebyshev	$(\frac{1}{2}, -\frac{1}{2})$
Legendre	$(0, 0)$
Jacobi $(1, 1)$	$(1, 1)$

Funding

This research received no external funding.

Conflicts of Interest

The authors declare no conflicts of interest.

References

[1] Abd-Elhameed, W.M., Machado, J.A. and Youssri, Y.H. *Hypergeometric fractional derivatives formula of shifted Chebyshev polynomials: Tau algorithm for a type of fractional delay differential equations*, Int. J. Nonlinear Sci. Numer. Simul., 23 (2022), 1253–1268.

[2] Abd-Elhameed, W.M., Al-Harbi, M.S., Amin, A.K. and Ahmed, H.M. *Spectral treatment of high-order Emden–Fowler equations based on modified Chebyshev polynomials*, Axioms, 12 (2023), 99.

[3] Abd-Elhameed, W.M., Alqubori, O.M. and Atta, A.G. *A collocation procedure for treating the time-fractional FitzHugh–Nagumo differential equation using shifted Lucas polynomials*, Mathematics, 12 (2024), 3672.

[4] Abd-Elhameed, W.M. and Alsuyuti, M.M. *New spectral algorithm for fractional delay pantograph equation using certain orthogonal generalized Chebyshev polynomials*, Commun. Nonlinear Sci. Numer. Simul., 141 (2025), 108479.

[5] Ahmed, H.M., Hafez, R.M. and Abd-Elhameed, W.M. *A computational strategy for nonlinear time-fractional generalized Kawahara equation using new eighth-kind Chebyshev operational matrices*, Phys. Scr., 99 (2024), 045250.

[6] Ahmed, H.M., Youssri, Y.H. and Abd-Elhameed, W.M. *Recursive and explicit formulas for expansion and connection coefficients in series of classical orthogonal polynomial products*, Contemp. Math., 5 (2024), 4836–4873.

[7] Arikoglu, A. and Ozkol, I. *Solutions of integral and integro-differential equation systems by using differential transform method*, Comput. Math. Appl., 56 (2008), 2411–2417.

[8] Babolian, E. and Biazar, J. *Solving the problem of biological species living together by Adomian decomposition method*, Math. Comput. Simul., 60(5–6) (2002), 427–432.

[9] Biazar, J. *Solution of systems of integral-differential equations by Adomian decomposition method*, Appl. Math. Comput., 168(2) (2005), 1232–1238.

[10] Biazar, J., Ghazvini, H. and Eslami, M. *He's homotopy perturbation method for systems of integro-differential equations*, Chaos Solitons Fractals, 39(3) (2009), 1253–1258.

[11] Canuto, C., Hussaini, M.Y., Quarteroni, A. and Zang, T.A. *Spectral methods: Fundamentals in single domains*, Springer, 2006.

[12] Dehghan, M. and Sabouri, M. *A Legendre spectral element method on a large spatial domain to solve the predator–prey system modeling interacting populations*, Appl. Math. Model., 37(3) (2013), 1028–1038.

[13] Dehghan, M. and Shahini, M. *Rational pseudospectral approximation to the solution of a nonlinear integro-differential equation arising in modeling of the population growth*, Appl. Math. Model., 39(18) (2015), 5521–5530.

[14] Eslahchi, M.R., Dehghan, M. and Amani, S. *The third and fourth kinds of Chebyshev polynomials and best uniform approximation*, Math. Comput. Model., 55(5–6) (2012), 1746–1762.

[15] Fakhar-Izadi, F. and Dehghan, M. *An efficient pseudo-spectral Legendre–Galerkin method for solving a nonlinear partial integro-differential equation arising in population dynamics*, Math. Methods Appl. Sci., 36(12) (2013), 1485–1511.

[16] Guo, B.Y. and Wang, L.-L. *Jacobi approximations in non-uniformly Jacobi-weighted Sobolev spaces*, J. Approx. Theory, 128(1) (2004), 1–41.

[17] Hafez, R.M., Youssri, Y.H. and Atta, A.G. *Jacobi rational operational approach for time-fractional sub-diffusion equation on a semi-infinite domain*, Contemp. Math., 4(4) (2023), 853–876.

[18] Hafez, R.M. and Youssri, Y.H. *Review on Jacobi-Galerkin spectral method for linear PDEs in applied mathematics*, Contemp. Math., 5(2) (2024), 2051–2088.

[19] Jerri, A.J. *Introduction to integral equations with applications*, John Wiley & Sons, 1999.

[20] Maleknejad, K. and Tavassoli Kajani, M. *Solving linear integro-differential equation system by Galerkin methods with hybrid functions*, Appl. Math. Comput., 159(3) (2004), 603–612.

[21] Maleknejad, K., Basirat, B. and Hashemizadeh, E. *A Bernstein operational matrix approach for solving a system of high order linear Volterra–Fredholm integro-differential equations*, Math. Comput. Model., 55(3–4) (2012), 1363–1372.

[22] Saeidy, M., Matinfar, M. and Vahidi, J. *Analytical solution of BVPs for fourth-order integro-differential equations by using homotopy analysis method*, Int. J. Nonlinear Sci., 9(4) (2010), 414–421.

[23] Sahu, P.K. and Saha Ray, S. *Numerical solutions for the system of Fredholm integral equations of second kind by a new approach involving semiorthogonal B-spline wavelet collocation method*, Appl. Math. Comput., 234 (2014), 368–379.

[24] Sahu, P.K. and Saha Ray, S. *Two-dimensional Legendre wavelet method for the numerical solutions of fuzzy integro-differential equations*, J. Intell. Fuzzy Syst., 28(3) (2015), 1271–1279.

[25] Sahu, P.K. and Saha Ray, S. *Legendre wavelets operational method for the numerical solutions of nonlinear Volterra integro-differential equations system*, Appl. Math. Comput., 256 (2015), 715–723.

[26] Sahu, P.K. and Saha Ray, S. *Numerical solutions for Volterra integro-differential forms of Lane–Emden equations of first and second kind using Legendre multi-wavelets*, Electron. J. Differ. Equ., 2015(28) (2015), 1–11.

[27] Sahu, P.K. and Saha Ray, S. *Legendre spectral collocation method for the solution of the model describing biological species living together*, J. Comput. Appl. Math., 296 (2016), 47–55.

[28] Sayed, S.M., Mohamed, A.S., Abo-Eldahab, E.M. and Youssri, Y.H. *Alleviated shifted Gegenbauer spectral method for ordinary and fractional differential equations*, Contemp. Math., 5(2) (2024), 1344–1370.

[29] Shakeri, F. and Dehghan, M. *Solution of a model describing biological species living together using the variational iteration method*, Math. Comput. Model., 48(5–6) (2008), 685–699.

[30] Shen, J., Tang, T. and Wang, L.-L. *Spectral methods: Algorithms, analysis and applications*, Springer Series in Computational Mathematics, Vol. 41, Springer, (2011).

[31] Szegő, G. Orthogonal Polynomials, 4th ed., American Mathematical Society Colloquium Publications, Vol. 23, 4th ed., (1975).

[32] Tomar, S. and Dhama, S. *An effective technique for solving a model describing biological species living together*, in Computational Methods for Biological Models, Springer Nature Singapore., 1109, (2023), 25–52.

[33] Turkyilmazoglu, M. *High-order nonlinear Volterra–Fredholm–Hammerstein integro-differential equations and their effective computation*, Appl. Math. Comput., 247 (2014), 410–416.

[34] Turkyilmazoglu, M. *Solution of initial and boundary value problems by an effective accurate method*, Int. J. Comput. Methods., 14(6) (2017), 1750069.

[35] Turkyilmazoglu, M. *Optimization by the convergence control parameter in iterative methods*, J. Appl. Math. Comput. Mech., 23(2) (2024), 105–116.

[36] Vasconcelos, P.B., Matos, J.M.A. and Trindade, M.S. *Spectral Lanczos' tau method for systems of nonlinear integro-differential equations*, in Integral Methods in Science and Engineering, Birkhäuser., 1 (2017), 305–314.

[37] Wang, H., Fu, H.M., Zhang, H.F. and Hu, Z.Q. *A practical thermodynamic method to calculate the best glass-forming composition for bulk metallic glasses*, Int. J. Nonlinear Sci. Numer. Simul., 8(2) (2007), 171–178.

[38] Wang, S.Q. and He, J.H. *Variational iteration method for solving integro-differential equations*, Phys. Lett. A, 367(3) (2007), 188–191.

[39] Wazwaz, A.M. *Linear and nonlinear integral equations: Methods and applications*, Springer, 2011.

[40] Xu, L., He, J.H. and Liu, Y. *Electrospun nanoporous spheres with Chinese drug*, Int. J. Nonlinear Sci. Numer. Simul., 8(2) (2007), 199–202.

[41] Yang, Y. and Chen, Y. *Spectral collocation methods for nonlinear Volterra integro-differential equations with weakly singular kernels*, Bull. Malays. Math. Sci. Soc., 42(1) (2019), 297–314.

[42] Youssri, Y.H. and Atta, A.G. *Radical Petrov–Galerkin approach for the time-fractional KdV–Burgers' equation*, Math. Comput. Appl., 29(6) (2024), 107.

[43] Youssri, Y.H., Atta, A.G., Abu Waar, Z.Y. and Moustafa, M.O. *Petrov–Galerkin method for small deflections in fourth-order beam equations in civil engineering*, Nonlinear Eng., 13(1) (2024), 20240022.

[44] Youssri, Y.H. and Atta, A.G. *Fejér-quadrature collocation algorithm for solving fractional integro-differential equations via Fibonacci polynomials*, Contemp. Math., 5 (2024), 296–308.